FULL PAPER

Dalton
www.rsc.org/dalton

Bis-(μ-saccharide-*C*-2-oxo) dinuclear Cu(II) complexes of 4,6-*O*-butylidene/ethylidene-*N*-(α-hydroxynaphthylidene/*o*-hydroxybenzylidene/5-bromo-*o*-hydroxybenzylidene)-β-D-glucopyranosylamine: structural aspects and data correlations †

Gudneppanavar Rajsekhar,[a] Ajay K. Sah,[a] Chebrolu P. Rao,*[a] Philippe Guionneau,[b] Muktha Bharathy[c] and T. N. GuruRow[c]

[a] *Bioinorganic Laboratory, Department of Chemistry, Indian Institute of Technology, Bombay, Mumbai-400 076, India. E-mail: cprao@chem.iitb.ac.in*

[b] *Institut de Chimie de la Matiere Condensee de Bordeaux, UPR 9048 CNRS, Pessac, France*

[c] *Solid State & Structural Chemistry Unit, Indian Institute of Science Bangalore-560 012, India*

Received 3rd April 2003, Accepted 6th June 2003
First published as an Advance Article on the web 25th June 2003

A total of five dinuclear copper complexes were synthesized using 4,6-*O*-butylidene/ethylidene-*N*-(α-hydroxynaphthylidene/*o*-hydroxybenzylidene/5-bromo-*o*-hydroxybenzylidene)-β-D-glucopyranosylamine. Upon recrystallisation from different solvents, *viz.*, dmso/MeOH/pyridine, seven different dinuclear copper complexes were generated, wherein the geometry around one or both of the copper centers changes from square planar to square pyramidal due to the binding of solvent molecule as the fifth ligand. The ligands and their complexes were characterized by elemental analysis, ^{1}H and ^{13}C NMR, FT-IR, FABMS, UV-Vis, optical rotation, CD and magnetic susceptibility measurements. The 3D structures of all the seven complexes were established by single crystal XRD. All the complexes are neutral and dinuclear with the metal to the glycosylamine ratio being 1 : 1. Each glycosylamine acts as tridentate with di-negative charge and bridges between the two copper centers through the C-2-oxo group of the saccharide part and further the coupling between the copper centers is antiferromagnetic. At least four different types of $Cu_2O_2^{2+}$ core structures were identified depending upon the presence or absence of a fifth ligand at the Cu(II) center. The β-$^{4}C_1$-pyranose form of the glycosylamine is retained even in complexes. The dinuclear complex is stabilized through intra-complex hydrogen bond interaction. The inter-molecular C–H ⋯ O interactions are manifested in the formation of a helical structure where the water molecules occupy the cavity. The structural diversity observed in the complexes and several data correlations are discussed in detail.

Introduction

It has been known for a long time that there exists interaction between carbohydrates and metal ions and such interactions are indeed very important in biological processes.[1] Copper ions, as centers at the active site of metallo-proteins play essential roles in biology,[2] such as electron transfer, oxidation and dioxygen transport. As simple saccharides do not bind to metal ions strongly, these are generally modified such that their binding capacity is enhanced. Thus the *o*-hydroxybenzylaldimines and α-hydroxynaphthylaldimines derived from amino sugars as ligands and their metal ion interactions with copper, nickel and iron are encountered in the literature.[3] Further the structures of Cu(II) complexes derived from glucose containing β-oxo-enamine ligands to result in the imine centers at the C-2 or C-5 or C-6 position were reported.[4] Ours was the first report on the copper structures derived from the saccharides having an imine center at the C-1 position.[5] We have been recently working on the synthesis, characterization and structure determination of protected saccharides, glycosyl amines, saccharide based imine containing (C1–N=C–) molecules and metal ion complexes[6] of these systems. In continuation with our on going efforts, herein we report the structural aspects and correlations among the data of a series of ligands (H_3L^1–H_3L^5) and their Cu(II) complexes leading to dibridged dinuclear complexes (**1**–**5**).

Experimental

D-Glucose, butyraldehyde and paraldehyde were procured from Aldrich Chemical Co., Fluka Chemical Co., and Loba Chemical Co., respectively. All solvents were purified immediately before use. Elemental analysis was carried out on ThermoQuest EA1112. FT-IR spectra were recorded on Nicolet Magna IR 550. The specific rotations were measured on a Jasco DIP-370 Digital polarimeter and in each case these were measured thrice using fresh solution and the mean value is reported. ^{1}H NMR spectra were recorded on a Varian VXR 300S spectrometer, whilst ^{13}C NMR spectra were recorded on a Bruker Avance DRX 500 spectrometer. CD studies were done on JASCO J-600 spectropolarimeter. UV-Vis studies were carried out on a UV-2101PC Shimadzu, UV-Vis scanning spectrophotometer. FAB mass spectra were recorded on a JEOL SX 102/DA-6000 mass spectrometer data system using argon/xenon (6 kV, 10 mA) as the FAB gas. The accelerating voltage was 10 kV, and the spectrum was recorded at room temperature with *m*-nitrobenzyl alcohol (NBA) as the matrix. 4,6-*O*-Butylidene-β-D-glucopyranosylamine and 4,6-*O*-ethylidene-β-D-glucopyranosylamine were synthesized as per the procedure reported by us[7] earlier. The ligands H_3L^2, H_3L^4 and H_3L^5 were synthesised and characterized by us[8,9] and the synthesis and characterization of **4** and **5** has been reported by us recently.[5] "BUY" and "ETY" refer to the butylidene and ethylidene moieties of the 4,6-*O*-protecting group, respectively.

Synthesis of ligands

4,6-*O*-Butylidene-*N*-(α-hydroxynaphthylidene)-β-D-glucopyranosylamine H_3L^1. The methanolic solution (25 cm^3) containing α-hydroxynaphthaldehyde (0.810 g, 4.70 mmol) and 4,6-*O*-butylidene-β-D-glucopyranosylamine (1.019 g, 4.67 mmol) was refluxed for 3 h. The yellow colored solid separated was filtered and washed with cold methanol, diethyl ether and dried under vacuum (1.40 g, 76.9%), mp 172–174 °C (Found: C,

† Electronic supplementary information (ESI) available: tables and figures. See http://www.rsc.org/suppdata/dt/b3/b303729k/

DOI: 10.1039/b303729k

64.8; H, 6.3; N, 3.3%; $C_{21}H_{25}NO_6$ requires C, 65.1; H, 6.5; N, 3.6%); ν_{max}/cm^{-1} 3486w (OH); 2961s, 2871s (C–H); 1633s (CH=N); 1544s (C=C); 1095s (C–O); $[\alpha]_D^{25}$ −17.5 ± 1.3°, (*c*1, Me_2SO); δ_H (300 MHz; solvent Me_2SO-d_6; standard $SiMe_4$) 0.89 (3 H, t, CH_3 of BUY), 1.37–1.41 (2 H, m, CH_2 of BUY), 1.53–1.56 (2 H, m, CH_2 of BUY), 3.26–3.51 (5 H, m, H-2, H-3, H-4, H-6), 4.09–4.11 (H, m, H-5), 4.60–4.62 (H, t, CH of BUY), 4.78 [(H, d, $^3J_{H1-H2}$ 8.6 Hz, H-1)], 5.37 (H, s, 3-OH or 2-OH), 5.70 (H, s, 3-OH or 2-OH), 6.85–8.13 (6 H, m, Ar–H), 9.23 (H, s, CH=N) and 14.28 (H, s, phenolic-OH); δ_C (500 MHz; solvent Me_2SO-d_6; standard $SiMe_4$) 67.2–91.9 (6 C, C-1–C-6), 101.3 (C, CH unit of BUY), 35.9 and 17.0 (2 C, CH_2s of BUY), 13.8 (C, CH_3 of BUY), 107.8–159.3 (10 C, Ar–C) and 173.4 (1 C, CH=N); *m*/*z* 388 ($[M + H]^+$, 100%), 387 ($[M^+]$, 60%).

4,6-*O*-Ethylidene-*N*-(α-hydroxynaphthylidene)-β-D-glucopyranosylamine H_3L^3. This was synthesised as per the procedure reported for H_3L^1, but by using α-hydroxynaphthaldehyde (0.850 g, 4.94 mmol) and 4,6-*O*-ethylidene-β-D-glucopyranosylamine (0.980 g, 4.78 mmol) (1.45 g, 84%), mp >200 °C (Found: C, 63.3; H, 5.7; N, 3.7%; $C_{19}H_{21}NO_6$ requires C, 63.5; H, 5.9; N, 3.9%); ν_{max}/cm^{-1} 3432w, 3213w (OH); 2989s, 2881s (C–H); 1637s (CH=N); 1535s (C=C); 1099s (C–O); $[\alpha]_D^{25}$ −30 ± 4°, (*c*1, Me_2SO); δ_H (300 MHz; solvent Me_2SO-d_6; standard $SiMe_4$) 1.27 (3 H, d, CH_3 of ETY), 3.26–3.52 (5 H, m, H-2, H-3, H-4, H-6), 4.07–4.10 (H, m, H-5), 4.69–4.75 (H, m, CH of ETY), 4.77 [(H, d, $^3J_{H1-H2}$ 8.66 Hz, H-1)], 5.41 (H, d, 3-OH or 2-OH), 5.70 (H, d, 3-OH or 2-OH), 6.85–8.13 (6 H, m, Ar–H), 9.23 (H, s, CH=N); δ_C (500 MHz; solvent Me_2SO-d_6; standard $SiMe_4$) 67.2–98.6 (6 C, C-1–C-6), 20.2 (C, CH_3 of ETY), 106.8–159.2 (10 C, Ar–C) and 173.3 (1 C, CH=N); *m*/*z* 360 ($[M + H]^+$, 55%), 359 ($[M^+]$, 25%).

General method for the synthesis of bis(μ-saccharide-C-2-oxo) dinuclear complexes

Equimolar concentration of the corresponding ligand and $Cu(OAc)_2.H_2O$ were stirred in methanol (30 cm^3) at room temperature for 10 h. The green colored compound precipitated was filtered and washed repeatedly with methanol, until the washings were colorless. Further they were washed with diethyl ether and dried under vacuum.

$[Cu(H_1L^1)]_2$ (1). The single crystals (**1a**) suitable for XRD were obtained by layering methanol into the concentrated solution of $[Cu(H_1L^1)]_2$ in pyridine (0.840 g, 94%), mp >200 °C (Found: C, 55.4; H, 5.2; N, 5.5%; $C_{42}H_{46}N_2O_{12}Cu_2$ requires C, 56.2; H, 5.6; N, 3.1%); ν_{max}/cm^{-1} 3372w (OH); 2960s, 2927s, 2871s (C–H); 1621s (CH=N); 1542s (C=C); 1096s (C–O); $[\alpha]_D^{25}$ −444 ± 20°, (*c*1, Me_2SO); *m*/*z* 898 ($[M]^+$, 70%), 510 (25%), 450 (35%) and 388 (35%).

$[Cu(H_1L^2)]_2$ (2). The single crystals (**2a**) suitable for XRD were obtained by layering methanol into the concentrated solution of $[Cu(H_1L^2)]_2$ in pyridine (0.715 g, 90%), mp >200 °C (Found: C, 50.6; H, 5.4; N, 5.3%; $C_{34}H_{42}N_2O_{12}Cu_2$ requires C, 51.1; H, 5.8; N, 3.5%); ν_{max}/cm^{-1} 3250w (OH); 2962s, 2872s (C–H); 1634s (CH=N); 1093s (C–O); $[\alpha]_D^{25}$ −172 ± 2.4°, (*c*1, Me_2SO); *m*/*z* 798 ($[M]^+$, 10%), 460 (10%), 400 (15%) and 338 (10%).

$[Cu(H_1L^3)]_2$ (3). The single crystals (**3a**) suitable for XRD were obtained by layering methanol into the concentrated solution of $[Cu(H_1L^3)]_2$ in Me_2SO (0.800 g, 95%), mp >200 °C (Found: C, 54.1; H, 4.9; N, 3.9%; $C_{38}H_{38}N_2O_{12}Cu_2$ requires C, 54.2; H, 5.0; N, 3.3%); ν_{max}/cm^{-1} 3259w (OH); 2877s (C–H); 1622s (CH=N); 1543s (C=C); 1090s (C–O); $[\alpha]_D^{25}$ −420 ± 5°, (*c*1, Me_2SO); *m*/*z* 842 ($[M]^+$, 70%), 483 (20%), 422 (40) and 360 (45). The FAB mass fragmentation observed in **4**: *m*/*z* 741 ($[M]^+$, 70%), 433 (5%), 369 (8%) and 307 (30%) and **5**: *m*/*z* 899 ($[M]^+$, 70%), 513 (10%), 448 (12%) and 388 (10%).

X-Ray crystallography

Single crystal X-ray diffraction data were collected for all the compounds on a Nonius Kappa CCD diffractometer in the ϕ scan + ω scan mode using Mo-Kα radiation. The structures **4a**, **5a** and **5b** were solved through SIR-92,[10] **1a**, **2a**, **3a** and **4b** through the SHELX-97[11] programs. All the structures were refined using the SHELXL-97 program packages. The diagrams were generated using the ORTEP3[12] program. Full matrix least-squares refinement with anisotropic thermal parameters for all non-hydrogen atoms was used. Hydroxyl hydrogen positions were recovered from the difference Fourier maps. The hydrogen atoms were treated as riding atoms with fixed thermal parameters. The structures **1a** refines well only in $P2_1$ and not in $P2_1/c$ wherein several reflections of *h*0*l* type, *l*-odd are present. The structure **2a** refines well only in $P\bar{1}$ and not in $P1$. Even though, the crystal structure **3a** is a close fit to $P2_1/c$, it does not refine well in this space group. Other details of data collection and structure refinement are provided in Table 1.

CCDC reference numbers 193689–193692, 210436–210438.

See http://www.rsc.org/suppdata/dt/b3/b303729k/ for crystallographic data in CIF or other electronic format.

Results and discussion

The ligands derived from 4,6-*O*-butylidene-β-D-glucopyranosylamine ($H_3L^1$and H_3L^2) and 4,6-*O*-ethylidene-β-D-glucopyranosylamine (H_3L^3, H_3L^4 and H_3L^5) and their Cu(II) complexes (**1**–**5**) are summarized in Scheme 1. Synthetic details and the characterization data of both of the ligands and the copper complexes are given in the experimental section, and the data of the elemental analyses and mass spectra support the formation of dinuclear copper complexes for all of **1**–**5**.

Mass spectral studies

The FAB mass spectra of all the ligands (H_3L^1–H_3L^5) and their dinuclear copper complexes (**1**–**5**) showed molecular ion peaks corresponding to their molecular weights as mentioned in the experimental section. The intensity ratio for the peaks M, M + 2 and M + 4 was 5.0 : 4.5 : 1.0 owing to the presence of copper in its two isotopic forms, *viz.*, 63 (69.17%) and 65 (30.83%). All these complexes exhibited a similar fragmentation pattern that complies with

$$Cu_2L_2 \xrightarrow{-L} Cu_2L \xrightarrow{-Cu} CuL \xrightarrow{-Cu} L$$

by the sequential loss of the ligand followed by the copper ion to result in a mononuclear complex unit (CuL) which in turn fragments to give the ligand unit (L) by the loss of the second copper ion, followed by the fragmentation of the ligand.

NMR studies

^1H and ^{13}C NMR spectra of all the ligands (H_3L^1 to H_3L^5) were measured. While the ligands exhibit diamagnetic spectra, the corresponding copper complexes, **1**–**5** showed paramagnetic ^1H NMR spectra.

Diamagnetic NMR spectra of ligands. Corresponding spectral data are given in the experimental section. The proton resonances of OH and NH_2 groups were further cross-checked by exchanging these with D_2O addition followed by spectral measurement. The peak corresponding to C-1–N*H*$_2$ observed in the precursors 4,6-*O*-butylidene/ethylidene-β-D-glucopyranosylamine at 2.350/2.360 ppm, disappear and new peak due to C*H*=N appears at 9.230–9.233 pm for α-hydroxynaphthylidene derivatives ($H_3L^1$and H_3L^3) and 8.570–8.586 ppm for *o*-hydroxybenzylidene derivatives (H_3L^2, H_3L^4 and H_3L^5), indicating that the NH_2 group present in the precursor

Table 1 Summary of crystallographic data for the complexes **1a**, **2a**, **3a**, **4a**, **4b**, **5a** and **5b**[a]

Compounds	1a	2a	3a	4a	4b	5a	5b
Empirical formula	$C_{52}H_{44}Cu_2N_4O_{12}$	$C_{44}H_{52}Cu_2N_4O_{14}$	$C_{38}H_{44}Cu_2N_2O_{16}$	$C_{31}H_{38}Cu_2N_2O_{13}S_{0.5}$	$C_{50}H_{54}Cu_2N_6O_{12}$	$C_{32}H_{40}Br_2Cu_2N_2O_{14}$	$C_{40}H_{42}Br_2Cu_2N_4O_{12}$
Temperature/K	293(2)	273(2)	293(2)	173(2)	173(2)	173(2)	173(2)
Crystal system	Monoclinic	Triclinic	Monoclinic	Orthorhombic	Orthorhombic	Triclinic	Triclinic
Space group	$P2_1$	$P1$	$P2_1$	$P2_12_12_1$	$P2_12_12_1$	$P1$	$P1$
a/Å	11.143(9)	9.740(3)	4.989(5)	13.184(1)	13.304(1)	10.488(1)	13.230(1)
b/Å	17.542(2)	11.316(3)	22.735(5)	13.683(1)	13.548(1)	12.677(1)	13.242(1)
c/Å	13.495(6)	12.034(4)	16.938(5)	35.411(2)	26.292(1)	14.761(1)	13.426(1)
α/°		96.2(1)				110.0(1)	104.8(1)
β/°	100.3(1)	107.7(1)	96.6(1)			102.1(1)	105.3(1)
γ/°		113.9(1)				91.2(1)	104.1(1)
Volume/Å^3	2595(2)	1114.0(6)	1908(2)	6388.0(8)	4738.9(5)	1792.4(3)	2066.6(3)
Z	2	1	2	8	4	2	2
Reflections collected	7885	12295	11907	31835	23119	15930	16737
Independent reflections	5570	9107	7071	10241	8318	9701	11552
R_{int}	0.0897	0.0320	0.0455	0.0556	0.0793	0.0337	0.0546
Final R_1 [$I > 2\sigma(I)$	0.0704	0.0376	0.0485	0.0449	0.0535	0.0294	0.0621
Final wR_2 [$I > 2\sigma(I)$	0.1506	0.0861	0.1047	0.0761	0.0976	0.0697	0.1488
R_1 (all data)	0.1706	0.0460	0.0995	0.0588	0.0737	0.0322	0.0717
wR_2 (all data)	0.2000	0.089	0.1386	0.0798	0.1049	0.0711	0.1545

[a] $R_w = [\Sigma w(|F_o| - |F_c|^2/\Sigma w(|F_o|^2]^{1/2}$ $w = 1/\sigma F^2 + 1.00$.

glycosylamine is converted to imine in H_3L^1–H_3L^5. In all the ligands, C-1–*H* was found at 4.560–4.783 ppm with coupling constants of 8.1–8.7 Hz, respectively, supporting the presence of β-anomeric form in all these ligands. The presence of *C*H=N (163.3–173.4 ppm) and aromatic carbon resonances (106.0–160.2 ppm) observed in the spectra of these ligands support the condensation reaction that converted the Sacch-C-1–NH_2 group to Sacch-C1–N=CH–Ar in the product. Thus the conclusions derived based on ^{1}H NMR spectra are supported by the ^{13}C NMR spectral data.

Paramagnetic NMR spectra of the complexes. In the ^{1}H NMR spectra of the complexes, a one to one assignment could not be possible due to paramagnetic effects on the position and width of the peaks where the width of the peaks is shifted by about 10 fold. Thus the spectral peaks were spread in the range −10 to +60 ppm as exhibited in case of the copper complexes. Fig. S1† illustrates the differences observed in the ^{1}H NMR spectra of **2** and its precursor ligand, H_3L^2. While the proton of the imine group, –*H*C=N– exhibits a large down-field shift, those of the aromatic protons give peaks both in the down-field as well as in the up-field up to −10 ppm. The results are in agreement with those generally observed in the literature in case of compounds having –N=CH– functional groups.[13]

FT-IR spectra

The δ_{NH_2} vibration observed in the precursor glycosylamines in the region 1627–1628 cm^{-1} is absent from the spectra of H_3L^1 – H_3L^5 and instead a new peak corresponding to the $\nu_{C=N}$ vibration appeared at 1627–1637 cm^{-1}, supporting the formation of a Schiff base moiety. Comparison of the spectra of copper complexes (**1**–**5**) with the corresponding precursor ones revealed the formation of the respective complexes. A decrease in $\nu_{C=N}$ of about 5–10 cm^{-1} was observed, indicating the binding of the –C=N– moiety to the Cu(II) center. The changes observed in the ν_{OH} region of the spectra are indicative of the binding of the C-2–OH group *via* deprotonation of the hydroxyl group.

Optical rotation

Optical rotation data measured for both of the ligands and the corresponding copper complexes (**1**–**4**) are given in Table 2. Our studies clearly demonstrate that the reaction of ammonia with α-D-anomers, *viz.*, 4,6-*O*-ethylidene-α-D-glucopyranose (+68 ± 1.1°) and 4,6-*O*-butylidene-α-D-glucopyranose (+48 ± 1.1°) results in the formation of β-D-glycosylamine products, *viz.*, 4,6-*O*-ethylidene-β-D-glucopyranosylamine (−8.0 ± 1.1°) and 4,6-*O*-butylidene-β-D-glucopyranosylamine (−15 ± 1.5°). The presence of the β-anomeric form is confirmed based on our crystal structure of 4,6-*O*-butylidene-β-D-glucopyranosylamine.[8] When these β-D-glycosylamines were converted to the corresponding imine products, *viz.*, H_3L^1 (−17.5 ± 1.3°), H_3L^2 (−54 ± 2.4°), H_3L^3 (−30 ± 4°) and H_3L^4 (−70 ± 0.5°), the same anomeric form is maintained but with a higher negative rotation value when compared to the precursor glycosylamines. The anomeric forms in all the molecules are supported by the ^{1}H NMR coupling constants of the C1–H as reported in this paper.

The optical rotation of 4,6-*O*-ethylidene/butylidene-α-D-glucopyranose in solution changes gradually over a period of time due to mutarotation. However, in case of all other derivatives including those of metal complexes, there is hardly any difference in the optical rotation even when these were left in solution for long periods, indicating that mutarotation was not possible to any considerable extent owing to their stable C-1 configuration.

It is true that the anomeric carbon, C-1 contributes richly to the overall optical rotation of the compound and this overrides the contributions from C2 to C5 in aldohexoses. Since the configuration around C2 to C5 remains almost the same,

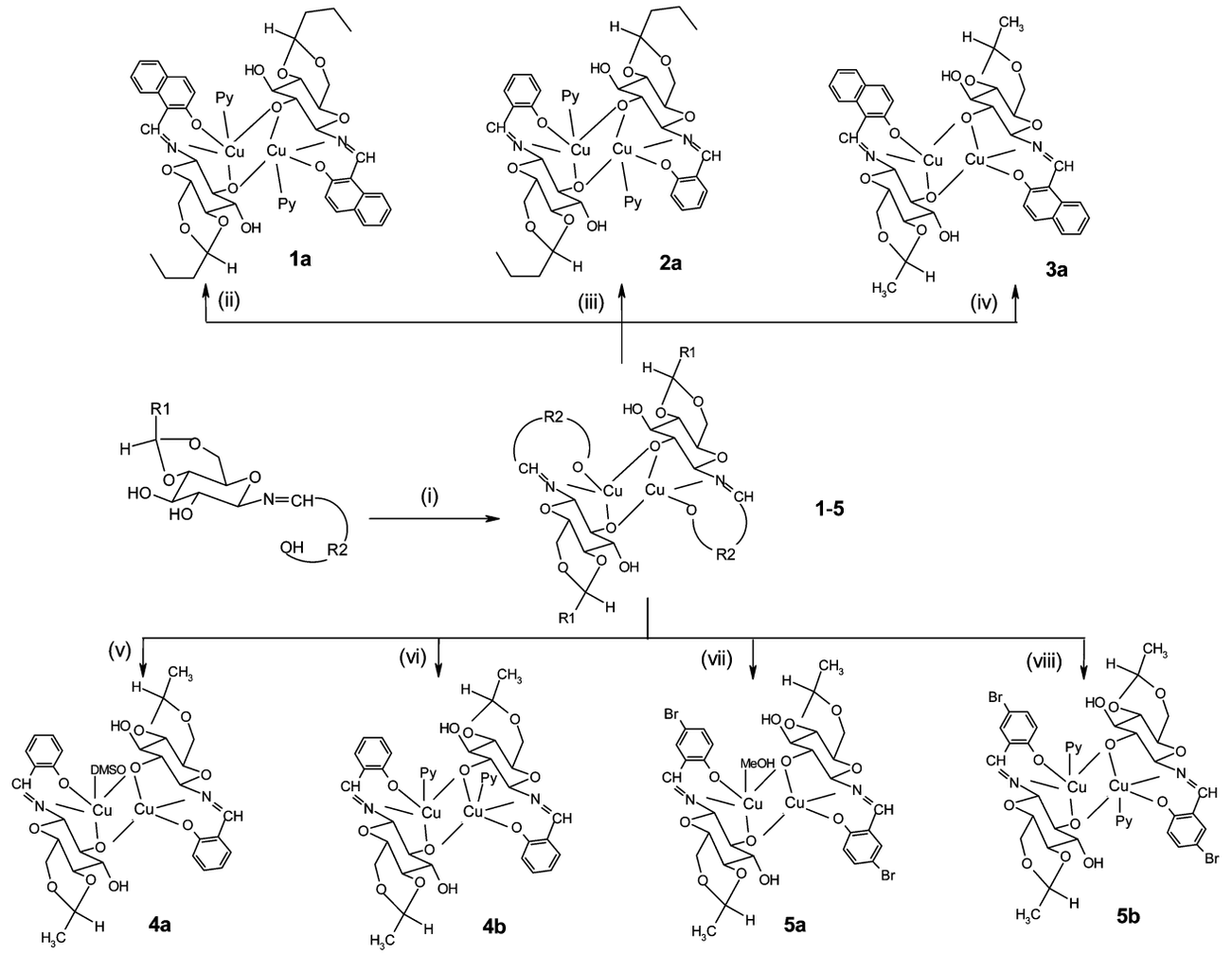

Scheme 1 The ligands are H_3L^1 when $R_1 = CH_3CH_2CH_2$- and R_2 = α-hydroxynaphthaldehyde; H_3L^2 when $R_1 = CH_3CH_2CH_2$- and R_2 = salicylaldehyde; H_3L^3 when $R_1 = CH_3$- and R_2 = α-hydroxynaphthaldehyde; H_3L^4 when $R_1 = CH_3$- and R_2 = salicylaldehyde; and H_3L^5 when $R_1 = CH_3$- and R_2 = 5-bromo-salicylaldehyde. **1**–**5** are their copper complexes. (i) MeOH/$Cu(OAc)_2 \cdot 4H_2O$; in the cases of (ii), (iii), (vi) and (viii), pyridine was used for recrystallisation; in the cases of (iv), (v) and (vii), DMSO/MeOH was used for recrystallisation.

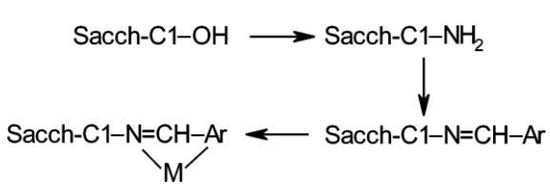

the large shift observed in case of their derivatives is due to the modification that took place at the anomeric C-1 center.

Thus such modifications bring changes in the polarizability at the anomeric center in terms of magnitude and direction. This indeed is noted from the observed optical rotations on going from Sacch-C1–OH to Sacch-C1–NH_2 to Sacch-C1–N=CH–Ar and all in the increasing negative sign of optical rotation. However a maximum negative shift was observed in optical rotation (−170 to −420°) when Sacch-C1–N=CH–Ar unit binds to the Cu(II) center. The magnitude of the rotation would, in addition, reflect on the contribution arising from C-2–O^- group that is indeed involved in bridging the two copper centers. From the data given in Table 2, it can be noted that the butylidene derivatives have more negative specific rotation values as compared to the corresponding ethylidene derivatives, indicating the possibility of higher stability (less prone to mutarotation) in case of the former. Further it can also be noted that the copper complexes are more stable than the corresponding organic derivatives, and among the Schiff's base derivatives, it is the *o*-hydroxybenzylidene derivatives that are more stable than the α-hydroxynaphthylidene derivatives. This aspect is also being noted through the browning of the reaction mixture when heated for long hours in the cases of the α-hydroxynaphthylidene derivatives (H_3L^1 and H_3L^3) but not in the cases of the *o*-hydroxybenzylidene derivatives (H_3L^2, H_3L^4 and H_3L^5).

UV-Visible absorption studies

The π⟶π* bands were shifted to longer wavelengths in case of H_3L^1 and H_3L^3 when compared to H_3L^2, H_3L^4 and H_3L^5 due to increase in the aromaticity in the case of former, owing to the presence of naphthyl moieties. In the copper complexes, a weak and broad band is observed in the region 616–640 nm corresponding to a d–d transition as shown in Fig. 1b (Fig. S2b†), and the corresponding molar ε values are greater with the α-hydroxynaphthylidene derivatives, **1** and **3** as compared to their *o*-hydroxybenzylidene counterparts, **2** and **4**. The absorption data are given in Table 2.

Both the d–d and charge transfer bands exhibit a shift in their position as well as in the intensity on going from solid to solution state where spectra were measured in dmf, dmso and pyridine. Thus there observed a red shift in the d–d transition by about 30 nm in case of pyridine and 20 nm in case of dmso solution as compared to dmf. However, the charge transfer band is red shifted only by about 15 nm in case of pyridine as compared to that of dmso or dmf. The intensities (mol^{-1} L cm^{-1}) of d–d and the charge transfer bands vary in their solution and the trend is, dmso (156, 8680) < dmf (204, 11120) < py (263, 11590). The spectral changes occurred in the solution as a function of the solvent indicates the binding of the solvent at

Table 2 Optical rotation, UV-Vis absorption and circular dichroism data for the ligands and their dinuclear copper complexes

Compound	Optical rotation/°	Absorbance/nm (ε/mol^{-1} L cm^{-1})	λ/nm (a/m°)
H_3L^1	−17.5 ± 1.3	422 (7080) 403 (7280) 366 (5220) 305 (11180)	352 (−4.52) 302 (+3.62)
H_3L^2	−54 ± 2.4	319 (6080) 262 (15060)	313 (−5.30) 271 (−12.10)
H_3L^3	−30 ± 4	422 (9750) 403 (10240) 364 (7480) 305 (16010)	355 (−3.90) 293 (+3.76)
H_3L^4	−70 ± 0.5	319 (7879) 261 (19812)	321 (−2.90) 269 (−7.95)
1	−444 ± 20	616 (398) 381 (20600) 320 (35400)	604 (+8.11) 426 (−5.93) 408 (−5.33) 370 (+16.61) 318 (−27.18) 278 (−52.30)
2	−172 ± 2.4	646 (156) 360 (8680)	602 (+4.30) 382 (−10.15) 346 (+11.99) 282 (+26.41)
3	−420 ± 5	641 (280) 380 (26800) 320 (45900)	610 (+3.63) 404 (−9.66) 368 (+13.62) 316 (−37.13) 278 (−61.23)
4	−136 ± 7	642 (183) 362 (21271) 274 (55513)	599 (+3.28) 385 (−7.79) 345 (+9.18) 283 (+19.17)

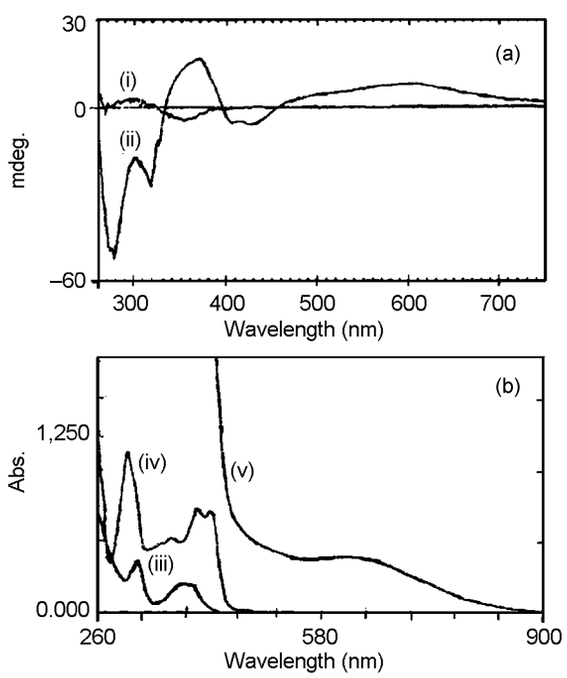

Fig. 1 (a) Circular dichroism spectra for H_3L^1 (10^{-2} M), (i) and **1** (10^{-3} M), (ii). (b) The corresponding UV-Visible absorption spectra for H_3L^1 (10^{-5} M), (iii), and **1** (10^{-4} M and 10^{-3} M), (iv). The spectrum labeled as (v) is an expanded version for **1** in the visible region.

Cu(II) centers by occupying its axial positions. Since the geometry changes from square planar to square pyramidal, the molecule loses the center of symmetry and hence there is more mixing in the p-orbitals of the ligand with the d-orbitals of the metal ion center resulting in enhanced intensites. The solid state reflectance spectra is similar to that observed in the DMSO solution indicating that the dinuclear copper complexes are stable even in solution.

Circular dichroism studies

The complexes exhibit a broad positive Cotton effect in the region of their d–d transitions. Representative CD spectra are given in Fig. 1a (Fig. S2a †), and the data are summarized in Table 2. The large Cotton effects observed, suggest the coordination of sugar moieties to the Cu(II) center. Since in all the complexes the magnitude and sign of Cotton effect in the d–d region are same, the binding core configuration around the metal ion is expected to be same in all the complexes. This indeed is further shown through the crystal structures of all of these complexes. Thus in the d–d transition, the absolute configuration around the metal center is a major contributor to the CD rather than the chelate ring conformation. The chelate ring conformations are discussed later in this paper. In the region 278–426 nm, several bands are observed with both positive and negative Cotton effects in case of the complexes as compared to that in the free ligand. This is probably due to the change in the chirality of the optical centers in the ligands as a vicinal effect after forming metal ion complexes.

Magnetic studies

The magnetic interaction between the two Cu(II) centers was studied as a function of temperature through measuring magnetic susceptibility. The plot of χ_M *vs.* T and μ_{eff}/μ_B *vs.* T are shown in Fig. 2 for **5a**. The interaction within the dinuclear unit

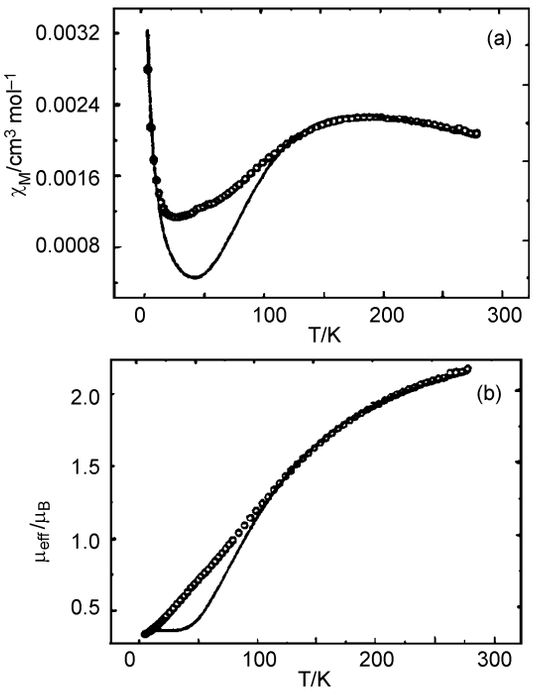

Fig. 2 Magnetic data for **5a** as a function of temperature: (a) χ_M/T, (b) μ_{eff}/T. The circles indicate the experimental points and the solid line a theoretical fitting curve.

is expected to be antiferromagnetic. The fit was performed with the usual expression for χ for a dinuclear unit with a paramagnetic impurity P, minimizing on the values between 2 and 10 K and above 75 K. The best-fit parameters were then: g = 2.09, $J = -20.6$ cm^{-1} and $P = 0.019$. The theoretical model does not make the fit well with that observed even after including zero-field splitting parameter in the calculations. The EPR spectral measurement of the solid did not provide any signal either at RT or at LNT indicating the presence of antiferromagnetic coupling between the two copper centers.

Molecular structures of 1a, 2a, 3a, 4a, 4b, 5a and 5b

All the complexes are neutral and dinuclear with the metal to the glycosylamine ratio being 1 : 1. Each glycosylamine acts as tridentate with di-negative charge and bridges between the two copper centers through the C-2–oxo group of the saccharide part, thus resulting in a di-bridging unit of $Cu_2O_2^{2+}$ core as shown in Scheme 1. The three binding sites of the glycosylamine ligand are phenolic/naphthylic-O$^-$, imine nitrogen and saccharide-C-2–O$^-$. Thus each copper center is tetra-coordinated to result in square planar geometry bound by NO_3 core. Such arrangement is observed in case of **3a** (Fig. 3a) and also in case of only one of the complex units present in the asymmetric unit of **4a** (Fig. S3†).

Geometry around Cu(II). However, during the crystallisation, either or both of the copper centers of the complex picks up a solvent molecule, *viz.*, pyridine, dmso or methanol and in turn the solvent molecule is bound to the Cu(II) center. In such cases the Cu(II) exhibits square-pyramidal geometry with either an N_2O_3 (in case of pyridine) or an NO_4 (in case of methanol or dmso) core. This resulted in the formation of complex units possessing five-coordination either at one or both of the Cu(II) centers, and when it is at both of the centers it resulted in either *syn*- or *anti*-orientations with respect to the dibridged Cu_2O_2 rhomb. All such structures are shown as ORTEP diagrams for **1a** (Fig. 3c), **2a** (Fig. S5†), **4a** (Fig. S4†), **4b** (Fig. S6†), **5a** (Fig. 3b) and **5b** (Fig. S7†). In the case of **4a** alone, the crystal structure exhibits two dinuclear units in each asymmetric unit cell, where one of the units is four-coordinated at both of the Cu(II)

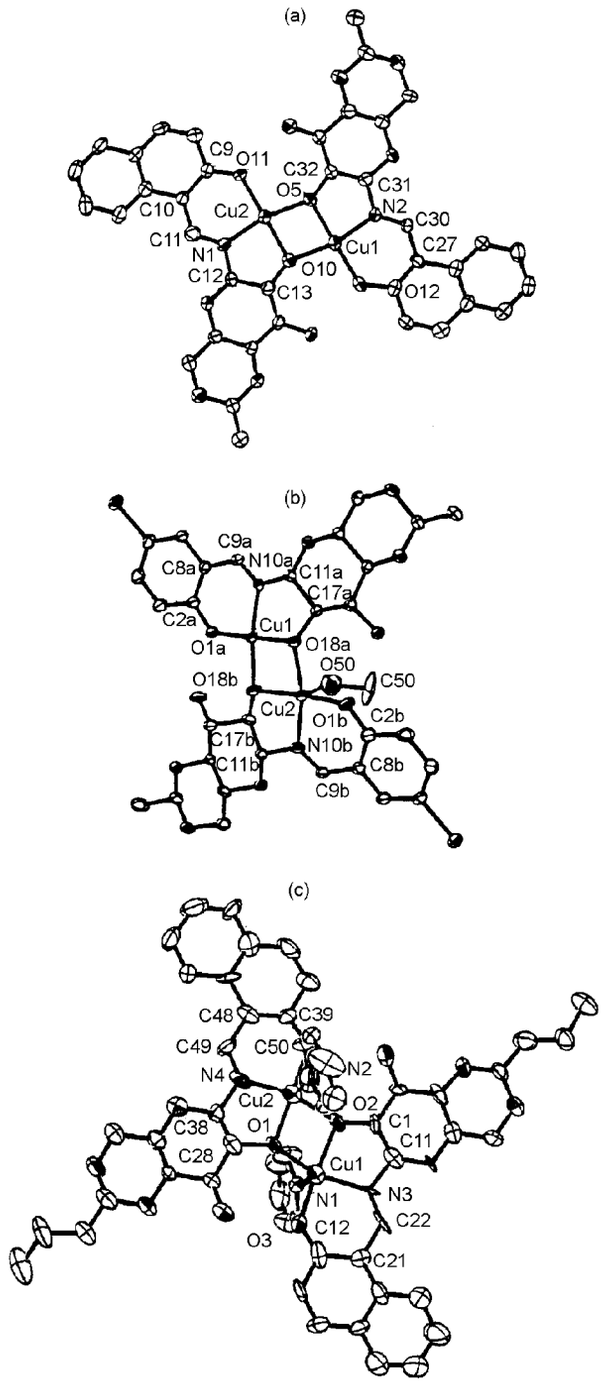

Fig. 3 (a) ORTEP structure for **3a**. The copper center in this structure is square planar. No fifth ligand is present on any copper centers. (b) ORTEP structure for **5a**. In this structure one of the copper centers has the square pyramidal geometry in which MeOH acts as the fifth ligand while the other has the square planar geometry. (c) ORTEP structure for **1a**. The co-ordination geometry around each copper center is square pyramidal and the pyridine molecules are oriented in a direction opposite to each other with respect to the Cu_2O_2 core.

centers (**4a**-1, Fig. S3†) and the other (**4a**-2, Fig. S4†) one is 5-coordinated, but at only one Cu(II) center of the dimeric unit. All our studies so far in this direction resulted in the complexes having either a four or five-coordinated Cu(II) center and none with a six-coordinated center.

Metric data of the primary coordination sphere. In the primary coordination sphere, the Cu–O_{phe} distance was found to be the minimum one with an average value of 1.90 Å, while those for Cu–N_{imine} and Cu–O_{sacch} are 1.94 and 1.96 Å, respectively. The selected bond distances in the primary co-ordination

Table 3 Selected bond distances (Å) in the primary coordination sphere of the dinuclear Cu-complexes

Bond	**1a**	**2a**	**3a**	**4a**[c]	**4b**	**5a**	**5b**
$Cu–N_{Imine}$	1.942(19) 1.940(2)	1.939(4) 1.968(4)	1.887(8) 1.901(8)	1.924(4)(A) 1.941(4)(A) 1.930(3)(B) 1.923(3)(B)	1.955(4) 1.972(4)	1.931(3) 1.940(3)	1.973(9) 1.937(8)
$Cu–N_{pyridine}$	2.332(14) 2.300(2)	2.291(4) 2.263(4)	— —	— —	2.264(4) 2.297(4)	— —	2.268(9) 2.310(9)
$Cu–O_{Solvent}$			—	2.383(4)[a](A)	—	2.428(5)[b]	—
$Cu–O_{phenolate}$	1.932(13) 1.971(14)	1.926(4) 1.906(4)	1.872(6) 1.866(7)	1.893(3)(A) 1.910(3)(A) 1.872(3)(B) 1.878(3)(B)	1.921(3) 1.913(3)	1.885(3) 1.911(3)	1.869(8) 1.934(7)
$Cu–O_{sacch}$	1.939(13) 1.964(11) 2.045(12) 1.987(14)	1.957(4) 1.977(3) 1.941(3) 1.990(4)	1.898(6) 1.941(6) 1.914(6) 1.950(6)	1.913(3)(A) 1.960(3)(A) 1.941(3)(A) 1.973(3)(A) 1.935(3)(B) 1.953(3)(B) 1.927(3)(B) 1.951(3)(B)	1.976(3) 1.970(3) 1.979(3) 2.011(3)	1.948(3) 1.915(3) 1.965(3) 1.957(3)	1.963(7) 1.923(7) 1.955(7) 1.960(7)
Cu–Cu	3.023(3)	3.009(1)	2.941(2)	2.899(1)(A) 2.962(1)(B)	2.977(1)	2.901(1)	2.984(2)

[a] Oxygen of dmso. [b] Oxygen of methanol. [c] There are two different dinuclear units in each asymmetric unit cell; A refers to **4a**-2 and B refers to **4a**-1.

sphere are summarized in the Table 3. The two molecules present in the asymmetric unit cell of **4a** exhibit variation in the metric data of the primary coordination sphere, including that of the Cu ··· Cu distance. The variations observed in the *trans*-angles *viz.*, 145.4 to 178.4° and the *cis*-angles *viz.*, 83.2 to 100.3° of the primary coordination sphere indicate distortion present in the geometry about the copper centers and the distortion follow an order, **2a** > **1a** > **5b** > **4b** > **4a** ≈ **3a** ≈ **5a**. This trend is indicative of high distortion in case of the dinuclear copper complexes where both of the copper centers are bound through one pyridine each. Further the observed trend fits well with that when the derivative is butylidene (**1a** and **2a**) the distortion about the metal center is high as compared to the corresponding ethylidene derivatives (**4b** and **5b**). Selected bond angles in the primary coordination sphere are given in Table 4.

Non-coordinated solvent molecules. Besides the two coordinated pyridine molecules, there exist two more pyridines in the asymmetric unit cell of **4b** which are neither coordinated to the copper center nor showing any interaction in the lattice. Thus, though in total four pyridine molecules are picked during the crystallisation only two of these approach close enough to the Cu(II) center in order to exhibit interaction, and hence no six coordination is observed at either Cu(II) center.

Structure of **5a** crystallises with two dinuclear copper complexes (**5a**-1 and **5a**-2) being present in the asymmetric unit cell where each of the dinuclear unit is associated with two MeOH molecules. Of the two methanol molecules one is weakly coordinated to one of the di-copper centers (2.347 Å in **5a**-1 and 2.428 Å in **5a**-2) and the second one shows a distance (3.211 Å in **5a**-1 and 3.354 Å in **5a**-2) that is beyond the sum of the van der Waal's radii with respect to the other copper center of the dimeric unit. Further these two MeOH molecules interact through a hydrogen bond. Thus it looks like that during the crystallisation two MeOH molecules are picked up, however, only one of these two could reach the copper center to exhibit an interaction.

Compound **4a**-2 crystallises with one non-coordinated water molecule. Oxygen of this water forms hydrogen bond interaction with the free –OH group of the glycosidic C-3 center where the O ··· O distance is 2.787 Å. Each asymmetric unit cell of **3a** crystallises with four water molecules and none of these form coordination with the Cu(II) center. However, one of these water molecules form a H-bond interaction with the free –OH group bound to the C-3 carbon of the glycosidic moiety like that observed in **4a**-2. Thus whenever water comes during crystallisation, the H_2O indeed is involved in a H-bond with the C-3–OH of the glycosylamine unit.

Diversity in dibridged Cu_2O_2 core units. Each copper center that is four-coordinated is found in a square planar (spl) environment and when a fifth ligand is present the geometry is found to be square pyramidal (spy). No dinuclear copper complex could be isolated where the Cu(II) center is six coordinated. Thus the dinuclear core structures identified in the present complexes can be fitted with the following geometries: (spl and spl), (spl and spy), (spy and spy with *syn*-orientation) and (spy and spy with *anti*-orientation) and the corresponding core structural diversity is shown in Fig. 4.

Stability of the di-nuclear structure. The di-nuclear structures seem to be specially stabilized owing to the presence of two O–H ··· O interactions developed between the two glycosylamine ligands within the dibridged Cu_2O_2 unit. It is the C-3–OH of one ligand acting as donor and the phenolic O^- of the neighbor ligand acting as acceptor that stabilizes these interactions. This has been observed in the crystal structures of all the di-nuclear copper complexes reported in this paper and is clearly shown in Fig. 5 for **4a**-1. The di-nuclear core was found to be retained even in solution.

Conformation and sugar puckering. In the glycosylamine ligands present in the complex, the saccharide moiety adopts a chair conformation in the β-$^4C_1$-pyranose form as judged from the Cremer–Pople puckering parameters[14] (Table S1†) computed using crystal structure data. While the θ value is observed around either 0 or 180°, the ϕ varies between 0 and 360°. All this produces only the iso-energetic forms of the $^4C_1$ chair conformation. The total puckering amplitude, Q and the distortion angle, θ were found to be close to an ideal cyclohexane chair form. Similar values were observed in the precursor glycosyl–Schiff base ligand, indicating that the $^4C_1$ conformation of the pyranose unit of saccharide is maintained even upon complex-

Table 4 Selected bond angles (°) in the coordination sphere of dinuclear copper complexes

	1a	**2a**	**3a**	**4a**(A)	**4a**(B)	**4b**	**5a**	**5b**
O_{Phe}–Cu–O_{Sacch}	170.6(6)	169.93(16)	100.3(3)	98.9(1)	175.3(2)	166.7(1)	98.5(1)	168.5(4)
	99.2(6)	98.51(15)	177.1(2)	178.4(1)	99.0(1)	97.8(1)	169.6(2)	98.9(3)
	170.9(6)	98.75(15)	177.6(2)	100.0(1)	175.9(2)	168.8(1)	177.4(2)	99.2(3)
	97.2(6)	172.95(19)	100.3(3)	173.0(2)	99.8(1)	98.7(1)	99.6(1)	169.9(3)
O_{Phe}–Cu–N_{Imine}	91.4(6)	93.60(16)	94.1(2)	93.6(2)	95.4(1)	92.5(2)	94.4(1)	93.7(4)
	90.0(7)	92.07(15)	93.6(2)	93.4(1)	95.0(1)	92.3(2)	92.8(2)	94.0(3)
N_{Imine}–Cu–O_{Sacch}	85.3(6)	152.70(14)	165.5(3)	167.3(2)	85.3(1)	83.6(1)	167.1(2)	152.1(4)
	153.2(6)	83.73(15)	85.6(3)	85.0(1)	165.6(1)	162.5(1)	84.6(1)	83.2(3)
	87.0(6)	85.12(16)	165.5(3)	84.1(1)	165.1(1)	83.7(2)	84.8(1)	159.6(3)
	148.4(6)	145.44(14)	85.8(3)	163.7(2)	84.6(1)	159.7(2)	166.2(2)	84.0(3)
Cu–O_{Sacch}–Cu	101.5(5)	98.66(15)	99.1(3)	96.5(1)	100.0(1)	97.6(1)	97.0(2)	100.6(3)
	97.1(5)	101.06(15)	100.0(3)	96.0(1)	99.3(1)	96.8(1)	95.7(1)	99.1(3)
O_{Sacch}–Cu–O_{Sacch}	81.1(5)	80.09(13)	80.0(2)	82.6(1)	80.3(1)	83.2(1)	81.9(1)	79.4(3)
	80.2(5)	80.17(14)	80.2(2)	81.5(1)	80.6(1)	82.3(1)	82.5(1)	80.3(3)
O_{Sacch}–Cu–N_{Py}	102.8(6)	95.83(15)	—	—	—	99.7(2)	—	94.1(3)
	103.7(7)	99.42(14)				95.1(2)		98.5(3)
	97.7(6)	100.11(15)				97.8(2)		95.7(3)
	97.7(6)	94.68(15)				93.0(2)		92.7(3)
O_{Phen}–Cu–N_{Py}	91.6(6)	94.24(16)	—	—	—	93.4(1)	—	97.4(4)
	91.4(7)	92.36(16)				93.3(2)		97.4(3)
N_{Imine}–Cu–N_{Py}	101.4(6)	103.30(16)	—	—	—	98.4(2)	—	104.4(3)
	106.9(7)	112.89(15)				103.4(2)		98.0(3)
O_{Sacch}–Cu–O_{Solv}				88.1(1)[a]	—	—	90.8(2)[b]	—
				88.4(1)[a]			94.4(2)[b]	
O_{Phen}–Cu–O_{Solv}				98.7(2)[a]	—	—	99.2(2)[b]	—
N_{Imine}–Cu–O_{Solv}				99.0(2)[a]	—	—	89.4(2)[b]	—

[a] Oxygen of DMSO. [b] Oxygen of methanol; A refers to **4a**-2 and B refers to **4a**-1.

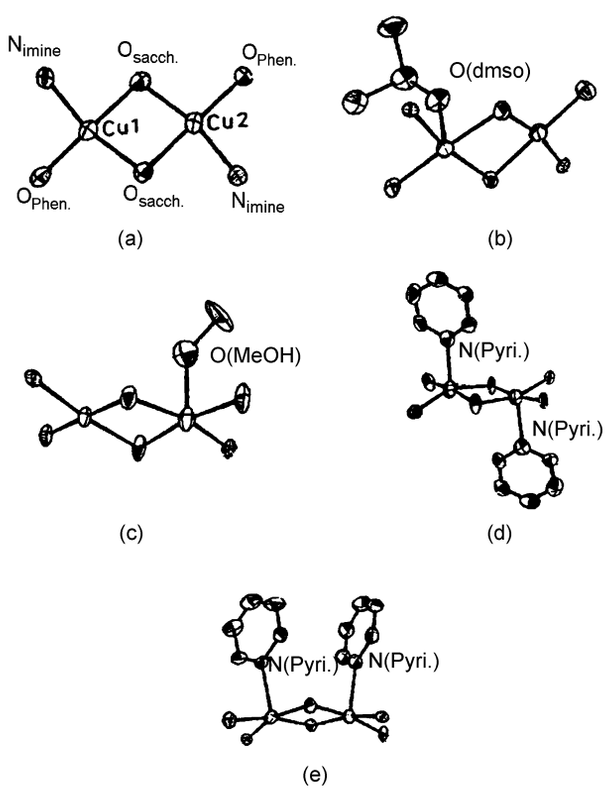

Fig. 4 Different types of binding cores observed in all the dinuclear copper complexes reported in this paper. The geometries at the Cu(II) centers of the dinuclear unit are: (a) (spl, spl); (b) (spy, spl); (c) (spl, spy); (d) (spy, spy; *anti*-type); (e) (spy, spy; *syn*-type), where spl is square planar and spy is square pyramidal.

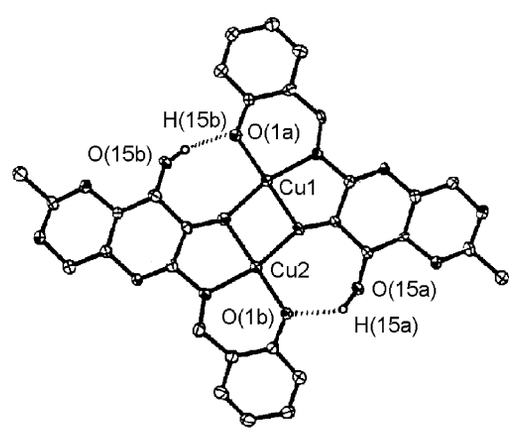

Fig. 5 Two intra-complex hydrogen bond interactions of the type O–H ··· O involved in stabilizing the dinuclear copper complex, as constructed from the crystal structure of **4a**-1.

ation. The six-membered ring connecting the 4,6-positions of the glycosylamine moiety also exhibits a $^4C_1$ conformation with marginally higher puckering amplitude and distortion angle (Table S1 †). The overall dinuclear unit exhibits a bowl shape and all the conformational features can be judged from the stereo-view (Fig. S8 †). Even the dihedral angles (Table S2 † for **4a**-1) are indicative of the β-$^4C_1$-pyranose form.

Five- and six-membered chelates. Each copper center in all these complexes is involved in forming one six-membered and another five-membered chelate. Conformational analysis of these chelates is computed based on the crystallographic data (Table S3 †). The five-membered chelates exhibit envelope and

half-chair conformations in almost equal proportions, but the pyridine bound ones show a preference for the half-chair over the envelope. The majority of the six-membered chelates exhibit either the boat or the skew-boat conformation with the least preference towards the chair form.

Deviation of the Cu(II) center. The Cu(II) ion fits well into the NO_3 plane in the complexes where there is no fifth ligand present. However, in the presence of a fifth ligand the Cu(II) center moves out of this NO_3 plane, in the direction of the fifth ligand, by about 0.1 to 0.3 Å depending upon the nature of this ligand, whether it is pyridine (~0.3 Å) or dmso/MeOH (~0.1 Å) (Table S4 †). It looks as if when the fifth ligand is bound, the Cu center acquires a certain amount of reduced character (more so in the case of Py as compared to dmso/MeOH) where in the copper ion size increases and hence is pushed out of the NO_3 plane. The average Cu–N_{py} is 2.291 Å and the average Cu–O_{solv} (dmso/MeOH) is 2.405 Å, indicating a stronger interaction in case of pyridine. Further the increase in the size of the copper ion can be justified from the increased Cu ··· Cu distance as observed from the crystal structures.

Cu ··· Cu separation in the dibridged Cu_2O_2 rhomb. The metric data were found to be normal and the Cu ··· Cu distance data rule out any possibility of having a bond between the two copper centers. In the complexes, **1**–**5** the Cu ··· Cu distance vary from 2.899(1) to 3.009(1) Å and plot between Cu ··· Cu distance and Cu–O_{sacch}–Cu angle exhibit an expected linear correlation with a positive slope (Fig. S9 †).

Hydrogen bonding interactions. All the dinuclear complexes show both intra- and intermolecular hydrogen bonds in almost equal number. The hydrogen bonds are of O–H ··· O and C–H ··· O type (Table S5 †). The intramolecular hydrogen bonds are however involved in stabilizing the dinuclear complex as explained in this paper. On an average, at least one intermolecular hydrogen bond per Cu–L unit is observed (indeed 2–3 hydrogen bonds per dimer, 2Cu + 2L). In case of free ligand, on an average, at least four intermolecular hydrogen bonds are observed per ligand.[8,9] The lower number of hydrogen bonds observed in the cases of the copper complexes could be attributed to the involvement of –C=N– and –C-2–OH units in the binding to the Cu(II) center. Thus the extensive intermolecular hydrogen bond interactions observed in case of the free glycosylamine ligand are decreased further upon complexation.

The intermolecular C–H ··· O type interactions arise between the aromatic C–H and the C-6–O of the glycosidic unit in the cases of **3a** and **4b**, and in the cases of **4a** and **5a**, these are observed between the glycosidic units. In the case of **1a** the C–H ··· O type interactions arise between the C–H of pyridine and C-3–O. These contacts are associated with longer hydrogen ··· acceptor (d = 2.4 to 2.6 Å) and donor ··· acceptor (D = 3.2 to 3.6 Å) distances indicating that such interactions are indeed weak ones as compared to the O–H ··· O type (d = 1.8 to 2.0 Å and D = 2.7 to 2.9 Å) interactions. These data are in agreement with that reported in the literature.[15] The correlation between the distance and the angle can be clearly understood from the D *vs.* θ and d *vs.* θ plots. From these plots it can be noted that the O–H ··· O and the C–H ··· O contacts are well separated and occupy almost two distinct regions corresponding to stronger and weaker interactions, respectively, as shown in Fig. 6 (also Fig. S10 †) through appropriate marking. Such weak interactions are responsible for the observed lattice structures in the dinuclear copper complexes reported in this paper.

Lattice structures

In the lattice of these complexes generally the dinuclear copper units are connected through C–H ··· O type of interactions to result in a structure close to that of helical type. In the case of **3a** alone one half of the dinuclear units show a C–H ··· O interaction between the naphthyl-C–H and C-6–O of the glycosyl moiety. The cavity formed between the two adjacent dinuclear units is filled with the water molecules (Fig. S11 †).

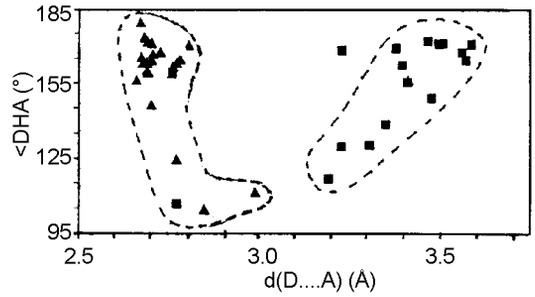

Fig. 6 Hydrogen bond data correlations in the dinuclear copper complexes: triangles represent O–H ··· O and squares represent C–H ··· O interactions. The D–θ scatter plot for the hydrogen bond interactions is shown. The data points present in each enclosure correspond to the same type of interaction.

Conclusions and correlations

All the reactions yield only di-nuclear complexes with a Cu_2O_2 core, where the copper center is found to have a square planar geometry and the two centers are anti-ferromagnetically coupled. Totally structures of seven such dinuclear complexes were established by single crystal XRD. The Cu ··· Cu distance exhibited a linear correlation with respect to the Cu–O–Cu angle (Fig. S9 †) among the complexes reported in this paper. No mononuclear complex could be isolated even when the reactions were carried out using 1 : 2 ratio of metal ion to the ligand. Indeed, the stability for such dinuclear complexes can be attributed to the presence of O–H ··· O type hydrogen bond interactions present between the two glycosylamine units of the same dinuclear unit (Fig. 5), reminiscent of that observed with the nickel–dimethylglyoxamato complex.

However when these complexes are crystallised from donor solvents, the geometry is changed from square planar to the five coordinated square-pyramidal Cu(II) one, but never a six-coordinated one. Whenever the solvent is weakly coordinating, *viz.*, dmso or MeOH, it binds only to one copper center of the dinuclear unit, but not to both of the centers. On the other hand, when the crystallisation was carried out from strongly coordinating pyridine, pyridine was always bound at both of the Cu(II) centers of the dinuclear unit resulting in a *syn*- or *anti*-orientation with respect to the Cu_2O_2 rhomb. This is manifested in the exhibition of structural diversity with four different core structures as shown in Fig. 4. Solution absorption studies also supported the interaction of the solvent molecules at the copper center. The absorption studies carried out in *N*,*N*-dimethylformamide using these dinuclear copper complexes as plausible catalysts in oxidizing 3,5-di-*tert*-butylcatechol did not yield encouraging results. Our observation of this is supported by the report of Reim and Krebs[16] who demonstrated that only the unsymmetrical dinuclear Cu(II) complexes indeed exhibit catecholase activity, while the symmetrical ones do not.

The changes observed in the optical rotations (Table 2) on going from one ligand to the other as well as on going from the ligand to the metal complexes are attributable to the influence exhibited by the type of 4,6-protection (ethylidene or butylidene), aromatic part of the imine present (*o*-hydroxybenzylidene or α-hydroxynaphthylidene) and the binding of the ligand itself on going from the free to that in the complex.

The intermolecular C–H ··· O interactions are manifested in the formation of a helical type chains and stacking of these resulted in interesting water filled cavities in the cases of **3a** and **4a** where the water molecules are stabilized through H-bond

interaction with the C-3–OH. The H-bond interaction data showed interpretable correlations (Fig. 6, also Fig. S10 †) among *d vs.* θ and *D vs.* θ, and exhibited well separated regions for C–H ··· O and O–H ··· O type interactions.

The β-anomeric- as well as $^4C_1$-pyranose forms continue to be present on going from the imine derivatives (H_3L^1–H_3L^5) to their copper complexes (**1**–**5**) as shown based on ^{1}H NMR spectra, specific rotation and crystal structures and supported by the Cremer and Pople puckering parameters.

Thus, the formation of stable, neutral dinuclear copper complexes possessing an interesting glyco-moiety is demonstrated beyond doubt, besides characterizing these compounds thoroughly. Owing to the presence of copper as well as optically active glyco-component that could show some specific interaction with the DNA back bone through hydrogen bonding as well as hydrophobic interactions, we presume that these complexes would be of interest in bioinorganic chemistry of DNA cleavage. Recently Cowan's group demonstrated the nuclease properties of copper aminoglycosides.[17]

Acknowledgements

CPR acknowledges the financial support from the Council of Scientific and Industrial Research (CSIR), New Delhi and the Department of Science and Technology, New Delhi. GR acknowledges the SRF fellowship from CSIR. We thank Professor Jan Reedijk of Leiden University for some magnetic work.

References

1 S. Yano, *Coord. Chem. Rev.*, 1988, **92**, 113–156; S. Angyal, *J. Adv. Carbohydr. Chem. Biochem.*, 1989, **47**, 1–43; D. M. Whitfield, S. Stojkovski and B. Sarkar, *Coord. Chem. Rev.*, 1993, **122**, 171–225.

2 E. I. Solomon, B. L. Hemming and D. E. Root, in *Bioinorganic Chemistry of Copper*, eds. K. D. Karlin and Z. Tyeklar, Chapman and Hill, London, 1993, pp. 3–20; H. Sigel, in *Metal ions in Biological Systems*, Marcel Dekker, New York, 1981, vol. 13, p. 394.

3 M. J. Adam and L. D. Hall, *Can. J. Chem.*, 1982, **60**(17), 2229–2237; M. Villagran, J. Costamagna, Y. B. Matsuhiro and S. Moya, *Bol. Soc. Chil. Quim.*, 1994, **39**(2), 121–128; D. Holland, D. A. Laidler, J. David and D. J. Milner, *J. Mol. Catal.*, 1981, **11**(1), 119–127; A. Fragoso, M. L. Kahn, A. Castineiras, J. P. Sutter, O. Kahn and R. Cao, *Chem. Commun.*, 2000, **16**, 1547–1548; L. D. Hall and T. K. Lim, *Carbohydr. Res.*, 1986, **148**(1), 13–23.

4 R. Wegner, M. Gottschaldt, H. Gorls, E. G. Jager and D. Klemm, *Angew. Chem., Int. Ed.*, 2000, **39**(3), 595–599; R. Wegner, M. Gottschaldt, H. Gorls, E. G. Jager and D. Klemm, *Chem. Eur. J.*, 2001, **7**(10), 2143–2157.

5 A. K. Sah, C. P. Rao, P. K. Saarenketo, K. Rissanen, G. A. Van Albada and J. Reedijk, *Chem. Lett.*, 2002, 348–349.

6 A. K. Sah, C. P. Rao, P. K. Saarenketo, E. K. Wegelius, K. Rissanen and E. Kolehmainen, *J. Chem. Soc., Dalton Trans.*, 2000, 3681–3687; A. K. Sah, C. P. Rao, P. K. Saarenketo, E. K. Wegelius, E. Kolehmainen and K. Rissanen, *Eur. J. Inorg. Chem.*, 2001, 2773–2781; T. M. Das, C. P. Rao and E. Kolehmainen, *Carbohydr. Res.*, 2001, **334**, 261–269; T. M. Das, C. P. Rao and E. Kolehmainen, *Carbohydr. Res.*, 2001, **335**, 151–158; A. K. Sah, C. P. Rao, P. K. Saarenketo and K. Rissanen, *Chem. Lett.*, 2001, 1296–1297; T. M. Das, C. P. Rao, E. Kolehmainen, R. M. Kadam and M. D. Sastry, *Carbohydr. Res.*, 2002, **337**, 289–296; A. K. Sah, C. P. Rao, P. K. Saarenketo, E. K. Wegelius, E. Kolehmainen and K. Rissanen, *Carbohydr. Res.*, 2001, **336**, 249–255.

7 G. Rajsekhar, C. P. Rao, P. K. Saarenketo, E. Kolehmainen and K. Rissanen, *Carbohydr. Res.*, 2002, **337**, 187–94; K. Linek, J. Alfoldi and M. Durindova, *Chem. Pap.*, 1993, **47**, 247–250.

8 G. Rajsekhar, U. B. Gangadharmath, C. P. Rao, P. Guionneau, P. K. Saarenketo and K. Rissanen, *Carbohydr. Res.*, 2002, **337**, 1477–1484.

9 A. K. Sah, C. P. Rao, P. K. Saarenketo, E. Kolehmainen and K. Rissanen, *Carbohydr. Res.*, 2001, **335**, 33–43; A. K. Sah, C. P. Rao, P. K. Saarenketo and K. Rissanen, *Carbohydr. Res.*, 2002, **337**, 79–82.

10 A. Altmore, G. Cascarano, C. Giacovazzo and A. Guagliardi, A program for crystal structure solution, *J. Appl. Crystallogr.*, 1993, **26**, 343–350.

11 G. M. Sheldrick, SHELX-97, Programs for Crystal structure Analysis (Release97-2), University of Göttingen, Germany, 1997.

12 L. J. Farrugia, *J. Appl. Crystallogr.*, 1997, **30**, 565.

13 S. Edward, S. Andrzej, B. Magdalena and L. Erik, *Polyhedron*, 2002, **21**(27–28), 2711–2717; M. Maekawa, S. Kitagawa, M. Munakata and H. Masuda, *Inorg. Chem.*, 1989, **28**, 1904–1909; P. K. Mandal and P. T. Manoharan, *Inorg. Chem.*, 1995, **34**, 270–277; N. N. Murthy, K. D. Karlin, I. Bertini and C. Luchinat, *J. Am. Chem. Soc.*, 1997, **119**, 2156–62.

14 D. Cremer, *Acta Crystallogr., Sect. B*, 1984, **40**, 498–500; D. Cremer and J. Pople, *J. Am. Chem. Soc.*, 1975, **97**, 1354–1358.

15 G. R. Desiraju and T. Steiner, *The Weak Hydrogen Bond in Structural Chemistry and Biology*, Oxford University Press Inc., New York, 1999.

16 J. Reim and B. Krebs, *J. Chem. Soc., Dalton Trans.*, 1997, 3793–3804.

17 A. Sreedhara, J. D. Freed and J. A. Cowan, *J. Am. Chem. Soc.*, 2000, **122**, 8814–8824; J. A. Cowan, *Indian J. Chem., Sect. A*, 2002, **41**, 65–72.